https://doi.org/10.1051/e3sconf/202124606010

Study of a water-source CO_2 heat pump for residential use: experimental discharge pressure control and performance analysis

Yantong Li*, *Natasa* Nord, *Inge Håvard* Rekstad, *Stein Kristian* Skånøy, *Lars Konrad* Sørensen

Department of Energy and Process Engineering, Norwegian University of Science and Technology, Trondheim, Norway

Abstract The heat pumps with the refrigerant of carbon dioxide (CO_2), i.e., CO_2 heat pumps, have the merits of low price and environmentally friendliness in comparison with those with traditional refrigerants, e.g., hydrochlorofluorocarbons and chlorofluorocarbons. Current studies mainly focused on the air-source CO_2 heat pumps, while investigations about the CO_2 heat pumps gaining heat or cold energy from different mediums, e.g., water, are lacking. In addition, although few studies presented the investigations on the discharge pressure of the CO_2 heat pumps (e.g., investigations of optimal discharge pressure), how to realize the effective discharge pressure control in the experimental conditions is still lacking. To remedy these knowledge gaps, this study presented an experimental investigation of a water-source CO_2 heat pump for residential use. A PI controller was used to maintain the fixed discharge pressure by adjusting the opening of the electronic expansion valve. The dynamic performance of the CO_2 heat pump in the typical discharge pressure of 7,200 to 8,400 kPa were analyzed. The results indicated that the method of using the PI controller to adjust the opening of the electronic expansion valve could effectively maintain the desired discharge pressure of the CO_2 heat pump in the experimental conditions.

1 Introduction

Energy demand is highly increasing due to rapid population increase and social development. Use of fossil fuels that causes environmental pollution is not advocated to deal with the energy crisis [1]. This motivates the development of technologies for increasing the use of renewable energy and energy efficiency. The corresponding goals have been formulated in European Union's "2030 Climate and Energy Framework": energy efficiency in 2030 will be 32.5% higher than that in 2021, and renewable energy share in 2030 will be increased to higher than 32% [2].

As an advanced energy-conversing technology, heat pumps utilize the thermal energy from the surrounding resource (e.g., water, air, and ground) for building heating or cooling purposes [3]. This results in the improvement of renewable energy utilization and increasing energy efficiency [4]. Thus, a lot of scholars have paid attention to the investigations of heat pumps. For instance, Rohde et al. [5] conducted the optimal control for an integrated energy system where the main components include heat pumps, solar collectors, and borehole thermal energy storage unit. The annual electricity use of the system was reduced by 5% when the developed optimal control strategy was used. Yu et al. [6] concluded that the heat pump systems were suitable for spacing heating purpose, because their energy-saving potential is considerable. Li et al. [7] presented an investigation of an outdoor swimming pool heating system for winter application. The air-source heat pump, solar collectors, and PCM storage tank were integrated in the investigated system. Based on the proposed main components sizing and multi-criterion methods, the optimal heating capacity of the air-source heat pumps, surface area of the solar collectors, and volume of the PCM storage tank were identified. However, the traditional heat pumps use the hydrochlorofluorocarbons and chlorofluorocarbons as the refrigerants, which causes the depletion of the ozone layer.

Using the CO_2 to replace the traditional refrigerants in heat pumps is an environmentally friendly task. In addition, CO_2 heat pumps have the advantage of offering higher than 80ºC water temperature [8]. These advantages motivate more studies about the CO_2 heat pumps. For instance, an experimental study indicated that the coefficient of performance (COP) of the CO_2 heat pump could be improved when the internal heat exchanger was applied [9]. The results presented in the Dai et al.'s study [10] indicated that the utilization of the direct dedicated mechanical subcooling technology could also improve the COP of the CO_2 heat pump. Further, Peng et al. [11] found that the use of vapor-injection technology could also enhance the COP of the CO_2 heat pump.

* Corresponding author: yantong.li@ntnu.no

The investigation of the optimal discharge pressure of the CO_2 heat pump is still a research hotspot [12]. For instance, Qi et al. [13] concluded that the optimal discharge pressure of the CO_2 heat pump was related to the outlet CO_2 temperature of the gas cooler. Song and Cao [14] found that the optimal discharge pressure of the CO_2 heat pump with the water precooler is higher than that of the standard CO_2 heat pump. Chen [15] developed a new correlation for the discharge pressure of the CO_2 heat pump on the basis of the pinch analysis. Although a few studies have presented the investigations on the discharge pressure of the CO_2 heat pumps, how to realize the effective discharge pressure control in the experimental conditions is still lacking.

This study therefore presents an experimental analysis of the discharge pressure control for a CO_2 heat pump. The PI controller is developed to maintain the constant discharge pressure of the CO_2 heat pump. Five cases with the discharge pressure of 7,200 kPa, 7,500 kPa, 7,800 kPa, 8,100 kPa, and 8,400 kPa were experimentally tested. The dynamic control performance of the case with the discharge pressure of 7,200 kPa was analyzed to demonstrate the reliability of the developed PI controller. In addition, the system COP for the heating purpose (*HCOP*), system COP for the cooling purpose (*CCOP*), and expansion valve opening in different discharge pressure were also analyzed.

The rest of this paper is organized as follows. Section 2 presents the experimental setup of the CO_2 heat pump. The definition of the system COP is introduced in Section 3. Section 4 gives the uncertainty analysis. Section 5 shows the results and analysis. Section 6 depicts the conclusions and future possible works.

2 Experimental setup

The experimental setup of the tested CO_2 heat pump plant is located in the Energy and Indoor Environment Laboratory at the Department of Energy and Process Engineering at the Norwegian University of Science and Technology. Figure 1 shows the diagram of the experimental setup for the CO_2 heat pump plant. This experimental setup consisted of the compressor, evaporator, expansion valve, fan coil, internal heat exchanger, gas cooler, liquid separator, pressure sensors, PI controller, pumps, and temperature sensors.

The compressor is produced by the Officine Mario Dorin Spa company, and its type is CD 300H. It has a rated rotation speed of 1,450 r/min and a rated displacement of 4.06×10^{-4} m^3/s. The gas cooler is produced by the Swep International AB company, and its type is B18H-30. The internal heat exchanger is produced by the KAORI Brazed Plate Heat Exchanger company, and its type is CO42-12W-S3. The evaporator is produced by the KAORI Brazed Plate Heat Exchanger company, and its type is CO95-40W-S37. The liquid separator is produced by the Skala AS company, and its type is VU8L. The expansion valve is produced by the Carel company, and its type is E2V18CS000. The discharge pressure was maintained at the fixed value by the developed PI controller adjusting the expansion valve opening. The proportional and integral values in the controller were set as 50% and 10s, respectively.

The mixture of 30% propylene glycol and 70% water was used as the heat transfer fluid at the evaporator side. The inlet and outlet temperature of the mixture in the evaporator were measured using the temperature sensor produced by Kamstrup with the accuracy of ±0.4%. The inlet and the outlet water temperature in the gas cooler were measured using the temperature sensor produced by the Carel company with the accuracy of ±(0.005×(measured temperature)+0.3)ºC. The volumetric flowrate of the mixture in the evaporator is measured by the flow meter produced by the GWF company with the accuracy of ±3%. The volumetric flowrate of the water in the gas cooler is measured by a variable-area flow meter with the accuracy of ±1% [16]. The evaporating and discharge pressure were measured by the pressure sensor produced by the Carel company with the accuracy of ±1%. The power of the compressor is measured by the power meter produced by the CARLO GAVAZZI company with the accuracy of ±1%.

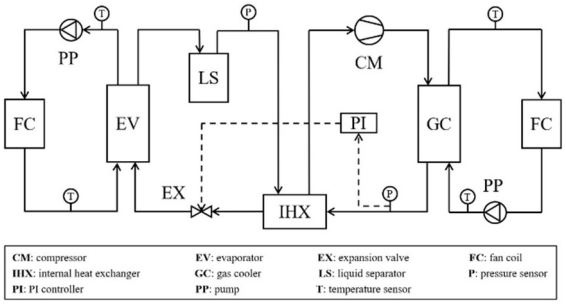

Figure 1. Experimental setup of the CO_2 heat pump plant.

3 System COP

The COP of the CO_2 heat pump system for both heating and cooling purposes were considered in this study. The system COP for the heating purpose (*HCOP*) was calculated as:

$$HCOP = Q,\dot{g}cr/P,cmr \quad (1)$$

where $Q,\dot{g}cr$ is the heat flow rate of the gas cooler and *P,cmr* is the compressor power.

The $Q,\dot{g}cr$ was determined as:

$$Q,\dot{g}cr = m,gcr \cdot c,gcr \cdot (T,gcr,o - T,gcr,i) \quad (2)$$

where *m,gcr* is the water mass flowrate of the gas cooler, *c,gcr* is the water specific heat of the gas cooler, *T,gcr,o* is the outlet water temperature of the gas cooler, and *T,gcr,i* is the inlet water temperature of the gas cooler.

The system COP for the cooling purpose (*CCOP*) was calculated as:

$$CCOP = Q,\dot{evp}/P,cmr \quad (3)$$

where $Q,\dot{evp}$ is the heat flow rate of the evaporator, which was determined as:

$$Q,\dot{evp} = m,evp \cdot c,evp \cdot (T,evp,i - T,evp,o) \quad (4)$$

where *m,evp* is the mass flowrate of the mixture of 30% propylene glycol and 70% water in the evaporator, *c,evp* is the specific heat of the mixture in the evaporator, *T,evp,i* is the inlet temperature of the mixture in the evaporator, and *T,evp,o* is the outlet temperature of the mixture in the evaporator.

4 Uncertainty analysis

The uncertainties of the measured variables were evaluated by a root-sum-square method as [17]:

$$u,mv = (\sum((\partial mv/\partial x,i) \times u,x,i)^2)^{0.5} \quad (5)$$

where *mv* is the evaluated variable, *x,i* is the i^{th} variable influencing the *mv*, *u,mv* is the calculated uncertainty of the *mv*, and *u,x,i* is the uncertainty of the *x,i*.

Based on this root-sum-square method, the uncertainties of the *HCOP* and *CCOP* were evaluated. The uncertainty of the *HCOP* (*u,HCOP*) was calculated as:

$$u,HCOP=(((\partial HCOP/\partial Q,gcr) \times u,Q,gcr)^2+((\partial HCOP/\partial P,cmr) \times u,P,cmr)^2)^{0.5} \quad (6)$$

where *u,Q,gcr* is the uncertainty of the $Q,\dot{g}cr$, and *u,P,cmr* is the uncertainty of the *P,cmr*. The *u,Q,gcr* was calculated as:

$$u,Q,gcr=(((\partial Q,gcr/\partial m,gcr) \times u,m,gcr)^2+((\partial Q,gcr/\partial T,gcr,o) \times u,T,gcr,o)^2+((\partial Q,gcr/\partial T,gcr,i) \times u,T,gcr,i)^2)^{0.5} \quad (7)$$

where *u,m,gcr* is the uncertainty of the *m,gcr*, *u,T,gcr,o* is the uncertainty of the *T,gcr,o*, and *u,T,gcr,i* is the uncertainty of the *T,gcr,i*.

The uncertainty of the *CCOP* (*u,CCOP*) was calculated as:

$$u,CCOP=(((\partial CCOP/\partial Q,evp) \times u,Q,evp)^2+((\partial CCOP/\partial P,cmr) \times u,P,cmr)^2)^{0.5} \quad (8)$$

where *u,Q,evp* is the uncertainty of the $Q,\dot{evp}$, which was calculated as:

$$u,Q,evp=(((\partial Q,evp/\partial m,evp) \times u,m,evp)^2+((\partial Q,evp/\partial T,evp,i) \times u,T,evp,i)^2+((\partial Q,evp/\partial T,evp,o) \times u,T,evp,o)^2)^{0.5} \quad (9)$$

where *u,m,evp* is the uncertainty of the *m,evp*, *u,T,evp,i* is the uncertainty of the *T,evp,i*, and *u,T,evp,o* is the uncertainty of the *T,evp,o*.

The average uncertainties of the calculated *HCOP* and *CCOP* are 3.93% and 3.92%, respectively.

5 Results and analysis

This section presents the experimental results for the typical cases with the discharge pressure of 7,200 kPa, 7,500 kPa, 7,800 kPa, 8,100 kPa, and 8,400 kPa. Table 1 presents the experimental results in different discharge pressure. The experimental results of the control performance in the case with the discharge pressure of 7,200 kPa were analyzed. The experimental results of the steady-state *HCOP*, *CCOP*, and expansion valve opening in different discharge pressure are also presented and analyzed.

Table 1. Experimental results in different discharge pressure.

Cases	Discharge pressure (kPa)	*m,gcr* (kg/s)	*T,gcr,o* (°C)	*T,gcr,i* (°C)	*m,evp* (kg/s)	*T,evp,o* (°C)	*T,evp,i* (°C)
1	7,200	0.067	41.0	27.9	0.194	17.6	20.4
2	7,500	0.067	42.8	27.3	0.174	14.0	17.9
3	7,800	0.067	45.2	28.7	0.182	14.7	19.0
4	8,100	0.067	46.6	28.9	0.187	14.1	18.5
5	8,400	0.067	47.2	28.3	0.186	12.7	17.3

5.1 Analysis of discharge pressure control

This section presents an example, in which the discharge pressure of the CO_2 heat pump was maintained at 7,200 kPa by the PI controller, to demonstrate the control performance of the system. Figure 2 shows the experimental results for the variations of discharge pressure, expansion valve opening, and evaporating pressure. In Figure 2 (a), at the beginning the discharge pressure rapidly increased to nearly 8,000 kPa, and then it suddenly decreased to nearly 7,050 kPa. At 80s, the discharge pressure increased to around 7,200 kPa. After this moment, the discharge pressure was well maintained at around 7,200 kPa until the end. In Figure 2 (b), at the beginning the expansion valve opening rapidly increased to 100%, and then it suddenly decreased to nearly 65%. The expansion valve opening fluctuated around 65% to maintain the discharge pressure at 7,200 kPa. Until nearly 240s, the fluctuation degree was reduced, and the expansion valve opening kept at 64% until the end. In Figure 2 (c), the evaporating pressure reduced with the increase of the time. The decreasing degree was reduced with the increase of the time. After 480s, the decreasing degree became very small, and the evaporating pressure was nearly constant as 5,000 kPa.

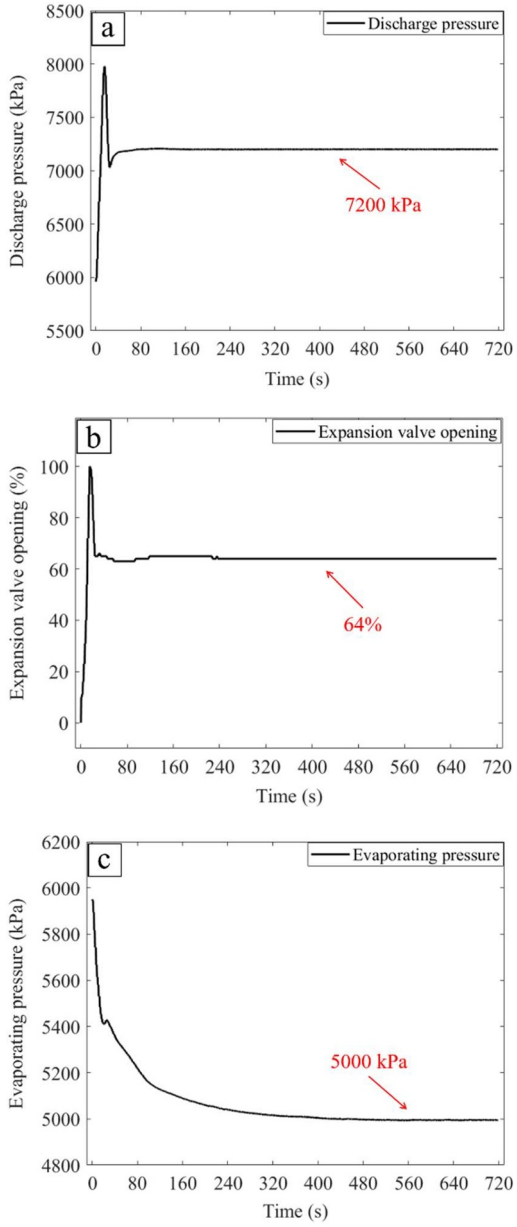

Figure 2. Experimental results of discharge pressure control: variation of (a) discharge pressure; (b) expansion valve opening; and (c) evaporating pressure.

5.2 Analysis of *HCOP*

Figure 3 presents the experimental results of *HCOP*, heat flow rate of the gas cooler ($Q, \dot{g}cr$), and compressor power (*P,cmr*) in typical cases with different discharge pressure. In Figure 3 (a), the *HCOP* was 3.52, 3.57, 3.63, 3.67, and 3.66, when the discharge pressure was fixed at 7,200 kPa, 7,500 kPa, 7,800 kPa, 8,100 kPa, and 8,400 kPa, respectively. Thus, the *HCOP* in the case with the discharge pressure of 8,100 kPa was higher than that in other cases. In Figure 3 (b), the $Q, \dot{g}cr$ increased with the increase of the discharge pressure. The $Q, \dot{g}cr$ was 3,650 W, 4,342 W, 4,601 W, 4,963 W, and 5,285 W, when the discharge pressure was fixed at 7,200 kPa, 7,500 kPa, 7,800 kPa, 8,100 kPa, and 8,400 kPa, respectively. In Figure 3 (c), the *P,cmr* increased with the increase of the discharge pressure. The *P,cmr* was 1,037 W, 1,215 W, 1,267 W, 1,353 W, and 1,444 W, when the discharge pressure was fixed at 7,200 kPa, 7,500 kPa, 7,800 kPa, 8,100 kPa, and 8,400 kPa, respectively. To conclude, from Figure 3, it is possible to notice that *HCOP* increased up to the discharge pressure of 8,100 kPa, regardless of the compressor power increase. This meant that the gas cooler heat rate had higher increase than the compressor power increase.

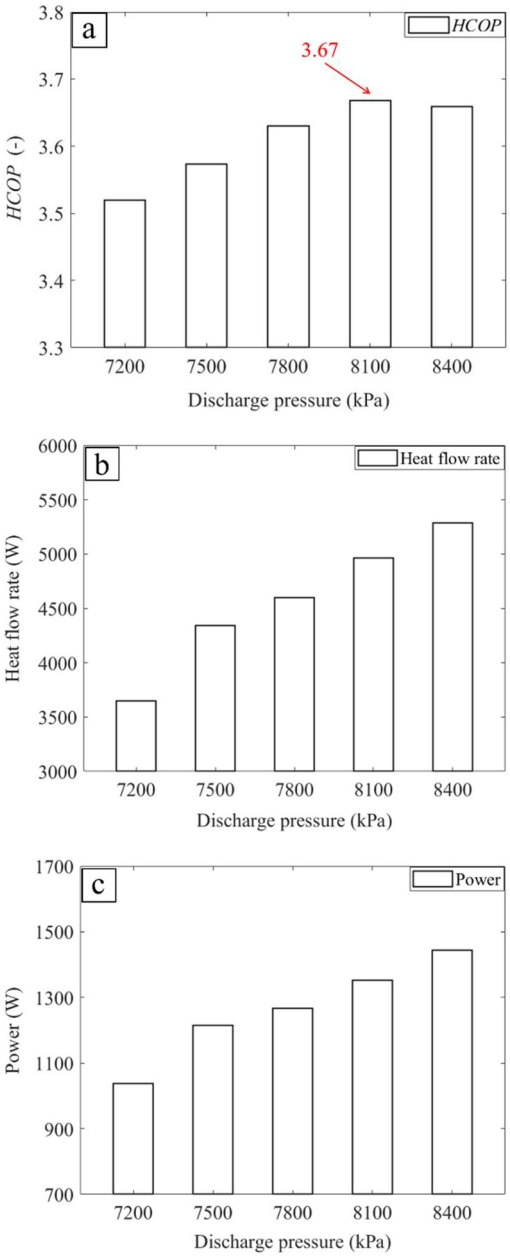

Figure 3. Experimental results of (a) *HCOP*; (b) heat flow rate in gas cooler; and (c) compressor power in typical cases with different discharge pressure.

5.3 Analysis of *CCOP*

Figure 4 presents the experimental results of *CCOP* and heat flow rate of the evaporator ($Q, \dot{evp}$) in typical cases with different discharge pressure. In Figure 4 (a), the *CCOP* was 1.96, 2.16, 2.36, 2.33, and 2.27, when the discharge pressure was fixed at 7,200 kPa, 7,500 kPa, 7,800 kPa, 8,100 kPa, and 8,400 kPa, respectively. Thus, the *CCOP* in the case with the discharge pressure of 7,800 kPa was higher than that in other cases. In Figure 4 (b), the $Q, \dot{evp}$ increased with the increase of the discharge pressure. The $Q, \dot{evp}$ was 2,036 W, 2,628 W, 2,986 W, 3,152 W, and 3,278 W, when the discharge pressure was fixed at 7,200 kPa, 7,500 kPa, 7,800 kPa, 8,100 kPa, and 8,400 kPa, respectively.

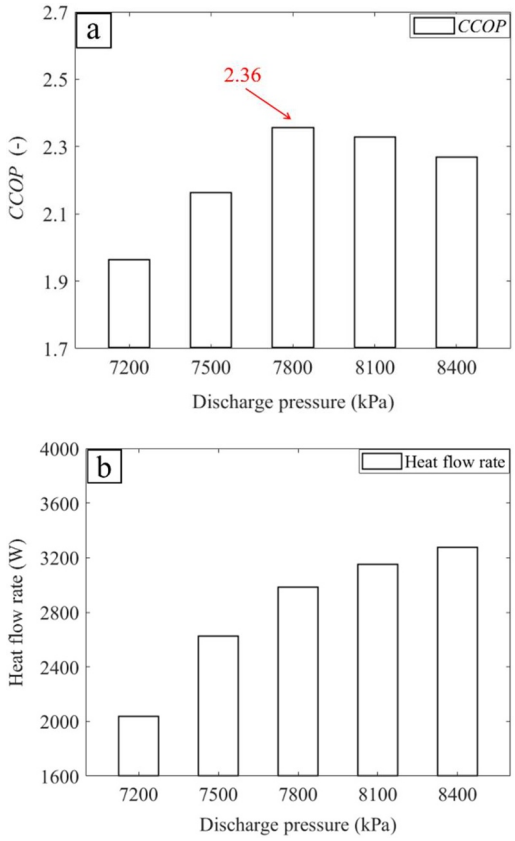

Figure 4. Experimental results of (a) *CCOP*; and (b) heat flow rate in evaporator in typical cases with different discharge pressure.

5.4 Analysis of expansion valve opening

Figure 5 presents the experimental results of the expansion valve opening in typical cases with different discharge pressure. It can be seen that the expansion valve opening reduced with the increase of the discharge pressure. The expansion valve opening was 64%, 35%, 33%, 26%, and 20%, when the discharge pressure is fixed at 7,200 kPa, 7,500 kPa, 7,800 kPa, 8,100 kPa, and 8,400 kPa, respectively.

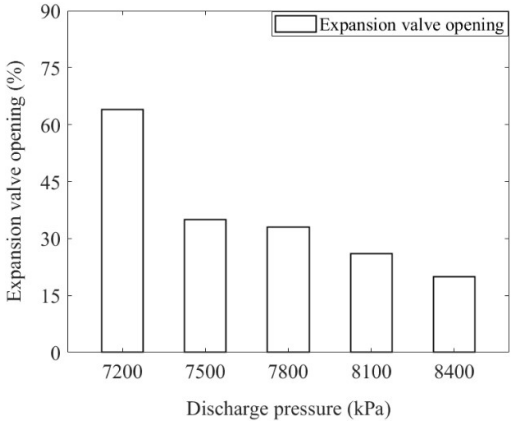

Figure 5. Experimental results of expansion valve opening in typical cases with different discharge pressure.

6 Conclusions and future possible works

An experimental analysis for the discharge pressure control of a water-source CO_2 heat pump was depicted in this study. The discharge pressure of the heat pump was maintained at the fixed value by the developed PI controller that could adjust the opening of the electronic expansion valve. To demonstrate the effectiveness of the discharge pressure control, the dynamic control performance of the CO_2 heat pump in the case with the discharge pressure of 7,200 kPa was analyzed. It was indicated that the developed PI controller could effectively maintain the discharge pressure at around 7,200 kPa in the experimental conditions, and thus the developed PI controller was reliable. In addition, the experimental results of the steady-state *HCOP*, *CCOP*, and expansion valve opening in typical cases with the discharge pressure of 7,200 kPa, 7,500 kPa, 7,800 kPa, 8,100 kPa, and 8,400 kPa were calculated and analyzed. It was found that the *HCOP* when the discharge pressure was fixed at 7,200 kPa, 7,500 kPa, 7,800 kPa, 8,100 kPa, and 8,400 kPa was 3.52, 3.57, 3.63, 3.67, and 3.66, respectively. The *CCOP* when the discharge pressure was fixed at 7,200 kPa, 7,500 kPa, 7,800 kPa, 8,100 kPa, and 8,400 kPa was 1.96, 2.16, 2.36, 2.33, and 2.27, respectively. The expansion valve opening when the discharge pressure was fixed at 7,200 kPa, 7,500 kPa, 7,800 kPa, 8,100 kPa, and 8,400 kPa was 64%, 35%, 33%, 26%, and 20%, respectively.

Future work may include the following topics. The performance comparisons between the air-source and water-source heat pump might be conducted using the established laboratory platform. An advanced controller might be developed to calculate the optimal discharge pressure setpoints for real applications. In addition, the experimental control performance under the varying operation conditions might be analyzed.

This project has received funding from the European Union's Horizon 2020 research and innovation programme under the Marie Sklodowska-Curie grant agreement No 895732 — ROCOCO2HP.

References

[1] Y. Li, N. Nord, Q. Xiao, T. Tereshchenko, "Building heating applications with phase change material: A comprehensive review," *J. Energy Storage*, vol. 31, 2020.

[2] Y. Li, N. Nord, G. Huang, X. Li, "Swimming pool heating technology: A state-of-the-art review," *Build. Simul.*, 2020.

[3] Y. Li, N. Zhang, Z. Ding, "Investigation on the energy performance of using air-source heat pump to charge PCM storage tank," *J. Energy Storage*, vol. 28, 2020.

[4] D. Rohde, T. Andresen, N. Nord, "Analysis of an integrated heating and cooling system for a building complex with focus on long–term thermal storage," *Appl. Therm. Eng.*, vol. 145, 2018.

[5] D. Rohde, B.R. Knudsen, T. Andresen, N. Nord, "Dynamic optimization of control setpoints for an integrated heating and cooling system with thermal energy storages," *Energy*, vol. 193, 2020.

[6] M. Yu, S. Li, X. Zhang, Y. Zhao, "Techno-economic analysis of air source heat pump combined with latent thermal energy storage applied for space heating in China," *Appl. Therm. Eng.*, vol. 185, 2021.

[7] Y. Li, N. Nord, H. Wu, Z. Yu, G. Huang, "A study on the integration of air-source heat pumps, solar collectors, and PCM tanks for outdoor swimming pools for winter application in subtropical climates," *J. Build. Perform. Simu.*, vol. 13, 2020.

[8] Y. Wang, Z. Ye, Y. Song, X. Yin, F. Cao, "Experimental investigation on the hot gas bypass defrosting in air source transcritical CO2 heat pump water heater," *Appl. Therm. Eng.*, vol. 178, 2020.

[9] F. Cao, Z. Ye, Y. Wang, "Experimental investigation on the influence of internal heat exchanger in a transcritical CO_2 heat pump water heater," *Appl. Therm. Eng.*, vol. 168, 2020.

[10] B. Dai, H. Qi, S. Liu, M. Ma, Z. Zhong, H. Li, et al., "Evaluation of transcritical CO_2 heat pump system integrated with mechanical subcooling by utilizing energy, exergy and economic methodologies for residential heating," *Energy Convers. Manag.*, vol. 192, 2019.

[11] X. Peng, D. Wang, G. Wang, Y. Yang, S. Xiang, "Numerical investigation on the heating performance of a transcritical CO_2 vapor-injection heat pump system," *Appl. Therm. Eng.*, vol. 166, 2020.

[12] F. Cao, Y. Song, M. Li, "Review on development of air source transcritical CO_2 heat pump systems using direct-heated type and recirculating-heated type," *Int. J. Refrig.*, vol. 104, 2019.

[13] P.-C. Qi, Y.-L. He, X.-L. Wang, X.-Z. Meng, "Experimental investigation of the optimal heat rejection pressure for a transcritical CO_2 heat pump water heater," *Appl. Therm. Eng.*, vol. 56, 2013.

[14] Y. Song, F. Cao, "The evaluation of optimal discharge pressure in a water-precooler-based transcritical CO_2 heat pump system," *Appl. Therm. Eng.*, vol. 131, 2018.

[15] Y.-G. Chen, "Optimal heat rejection pressure of CO2 heat pump water heaters based on pinch point analysis," *Int. J. Refrig.*, vol. 106, 2019.

[17] E. Toolbox, "Accuracy of variable-area flow meter,"https://www.engineeringtoolbox.com/flowmeters-accuaracy-d_657.html, 2020.

[18] R.J. Moffat, "Describing the uncertainties in experimental results," *Exp. Therm. Fluid Sci.*, vol. 1, 1988.